In Silico Screening and Designing Synthesis of Cinchona Alkaloids Derivatives as Potential Anticancer

Muhammad Hanafi [1*], Rosmalena [2], Vivitri Dewi Prasasty [3], Linar Zalinar Udin [1], Gian Primahana [1]

[1] Research Center for Chemistry, Indonesian Institute of Sciences, Puspiptek, Serpong, Indonesia

[2] Department of Medical Chemistry, Faculty of Medicine, University of Indonesia, Jakarta, Indonesia,

[3] Faculty of Biotechnology, Atma Jaya Catholic University of Indonesia, Jakarta, Indonesia

ABSTRACT

P-glycoprotein (P-gp) resistance in cancer cells decreases the intracellular accumulation of various anticancer drugs. This multidrug resistance (MDR) protein can be modulated by number of non-cytotoxic drugs. We have screened 30 cinchona alkaloids derivatives as a potent P-gp inhibitor agent *in silico*. Hereby, we report the highest potential inhibitions of P-gp is Cinchonidine isobutanoate through molecular docking approach with affinity energy -8.6 kcal/mol and inhibition constant, Ki is 4.89×10^{-7} M. Cinchonidine isobutanoate is also known has molecular weight below 500, Log P value 3.5, which is indicated violation free of Lipinski`s rule of five. Thus, Cinchonidine isobutanoate is the most potent compound as anticancer compare to other Cinchona alkaloids. Ultimately, we design Cinchonidine isobutanoate for further lead synthesis by using DBSA, act as a combined Brønsted acid-surfactant-catalyst (BASC) to obtain a high concentration of organic product by forming micellar aggregates which are very powerful catalytic application in a water environment.

INTRODUCTION

The progressive malignant cells resistance to cytotoxic drugs is one of the major issues for the failure of chemotherapy. The chemotherapeutic resistance has several mechanisms, i.e., 'multidrug resistance' (MDR), that involves an increased expression of the mdr1 gene, a 170 kDa glycoprotein called P-glycoprotein (P-gp) [1, 2]. The protein belongs to a large superfamily of highly conserved ATP-binding cassette proteins, facilitates the cellular efflux of various substances by reducing their intracellular concentration [3, 4, 5]. In normal cells of different tissues, such as biliary canaliculi, endothelium of the blood-brain barrier and bone marrow stromal cells, P-gp is known could act as a detoxifying agent by pumping toxins or xenobiotics out of these cells [6, 7]. It affects the absorption, distribution, and clearance of multidrug including cancer drugs and xenobiotics [8-11]. Overexpression of P-gp in cancer cells reduces intracellular accumulation of a broad range of anticancer medicinal products in the membrane bilayer [5, 12, 13].

In a search for more efficient P-gp inhibitors, we have screened 30 cinchona alkaloids as the potential anticancer through molecular docking and drug likeness evaluation. However, the crystal structure of human P-gp (hP-gp) is not available yet. The homology modeling of the human P-gp structure is built which its sequence is retrieved from Uniprot (Entry Code: P08183). Multidrug resistance protein 1A, a refined structure of mouse P-gp [14] is used as a template, and it is found 87.28% as the highest sequence similarity aligned with the human P-gp target. The structure refinement and structure validation have been done to obtain the high quality of the three-dimensional hP-gp structure.

The 3D structures demonstrated to be stable and trustworthy. Based on the 3D structure, the ligand binding modes of 3D structural diverse hP-gp binders were

*Corresponding author:
Muhammad Hanafi
Research Center for Chemistry, Indonesian Institute of Sciences
Jalan Raya Puspiptek – Serpong, Tangerang Selatan, Indonesia 15314
Email: hanafi124@yahoo.com

elucidated using molecular docking. Ligand binding free energies of the hP-gp binders were calculated using the free energy method and revealed that hP-gp could accommodate structurally diverse ligands having different electrostatic and hydrophobic properties. Docking method is an energy-based scoring function which identifies the energetically most favorable ligand conformation that binds to the protein target. Moreover, the best binding mode of cinchona alkaloid will be used as a model for synthesis and evaluated its biological activities both *in vitro* and *in vivo*.

MATERIALS AND METHODS

Protein structure preparation

The amino acid sequence of hP-gp (Entry Code: P08183) was retrieved from UNIPROT protein database. The 3D structure of protein hP-gp was generated by web-based SWISS-MODEL program. All homology modeling methods consist of the following four steps: (i) template selection; (ii) target-template alignment; (iii) model building; and (iv) model evaluation. These steps are iteratively repeated until a satisfying model structure is determined. The SWISS-MODEL web server approach can be described as rigid fragment assembly [15-18].

Protein structure refinement and validation

hP-gp 3D structure was checked by using Procheck [19] to validate its refined structural conformation. Ramachandran plot [20-23] and ERRAT [24] were used to analyze the allowed dihedral phi and psi rotation of amino acids in the protein backbones and the quality of refined 3D structure, respectively.
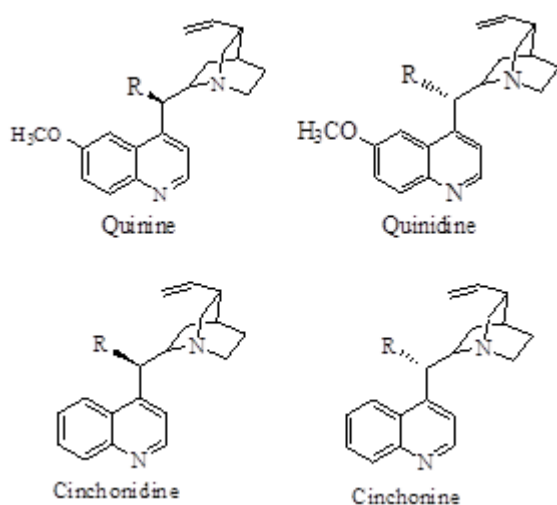

Figure 1. Structures of parental Cinchona alkaloids

Cinchona alkaloid derivative structures preparation

All 30 Cinchona alkaloid 3D structures were generated by ChemDraw Ultra 12.0 [25, 26] for the molecular docking experiments and their conformational energy was minimized by using a MMFF94 force field. 30 molecules of Cinchona alkaloids were designed by substituting the −R group positions of Cinchona (Table 1). The parental molecule structures of Cinchona alkaloids are depicted in Figure 1. The structures were scored based on their physicochemical properties under Chemicalize (ChemAxon) [27] and Molsoft [28] platforms. These physicochemical properties are essential for developing drug candidate at every stage from design to pre-clinical study.

Drug-likeness analysis of Cinchona alkaloids

Structures of 3D of Cinchona alkaloids were analyzed using a program based on the physicochemical properties, Molsoft - Drug Likeness. Physicochemical properties are important in rational drug design as the transition from early state development to pre- clinical trial applications.

Molecular docking analysis of hP-gp protein and Cinchona alkaloids

Molecular docking of hP-gp protein and Cinchona alkaloids was performed using AutoDock Vina. Autodock Vina is known to have high speed and accuracy, which is magnitude faster than AutoDock 4.2.

AutoDock Tools was utilized to prepare the input file as pdbqt format of hP-gp, also to set grid box to be resized and centered. Kollman charges and polar hydrogen atoms were added to hP-gp protein structure. The hP-gp protein cavity size was adjusted at $30 \times 30 \times 30$ in the dimensions size of x, y and z, respectively using 1,000 Å spacing. Ligands from Cinchona alkaloids were also required to be prepared as output pdbqt file formats using AutoDock Tools. The predicted energy affinity (kcal/mol), which indicates the strength of ligand binding to the receptor, is calculated based on the scoring function used in AutoDock Vina program. The scoring function in AutoDock Vina depends on the conformation-dependent part as a sum of intramolecular and intermolecular interactions, including effect steric, hydrogen bonding and hydrophobic interactions. It also depends on the number of rotatable and non-rotatable bonds between heavy atoms in the ligand. Each interaction including the interaction of effect steric, hydrogen bonding, hydrophobic and some rotatable bonds, is obtained as different weight in AutoDock Vina scoring

function [31].

RESULTS AND DISCUSSION

In investigating the anticancer potency of the Cinchona alkaloids, the chimeric enzyme was obtained and the structure was modeled followed by energy minimization. The model structure was subjected to molecular modeling analysis using Autodock Vina (The Script Institute). Autodock Vina is a well heuristic search algorithm which is based on guided differential evolution, which in turn is an algorithm that combines the differential evolution optimization technique and cavity prediction. The automatic cavity prediction along with automatic preparation of protein and ligand fully automates the entire benchmarking process.

The interactions resulted in this docking were found that Cinchona alkaloids exhibit excellent interactions with hP-gp in term of the ability in inhibiting this transmembrane efflux pump (Figure 2). Cinchonidine isobutanoate is found as the best inhibitor based on its affinity energy value is -8.6 kcal/mol compared to other Cin-

chona alkaloids (Table 2). Based on affinity energy values of other cinchona alkaloids which are derived from quinine, quinidine, cinchonine, and cinchonidine in two isomer forms have shown that all are low affinity when docked to P-gp.

The P-gp crystal structure opens its drug pathway at the level of the internal membrane process by lowering the intracellular concentrations of many drugs to sub-therapeutic levels by translocating them out of the cell. In the helical flanking site, the extended loops could mediate drug binding, which its function as hinges at the gated pathway [13, 29, 30]. The transitions of P-gp dynamics as it moved through conformations based on crystal structures of homologous ABCB1 proteins has been targeted in the previous study. We expanded our study by docking transport drug to natural inhibitors binding sites of P-gp in conformations. These results increase our understanding of the structure and function of this important molecule. Thus, based on the binding energy and hydrogen bond interaction, it can be confirmed that Cinchonidine isobutanoate inhibits the hu-

Table 1.   Compounds derived from parental Cinchona alkaloids were designed by substituting the —R group

No.	Compound	R-substitution	MW
1.	Quinine	-OH	324.18
2.	Quinine butanoate	-OC(O)CH2CH2CH3	364.22
3.	Quinine isobutanoate	-OC(O)CH(CH3)2	394.23
4.	Quinine isovalerate	-OC(O)CH2CH(CH3)2	408.24
5.	Quinine tiglate	-OC(O)C(CHCH2)(CH3)	406.23
6.	Quinidine	-OH	326.2
7.	Quinidine butanoate	-OC(O)CH2CH2CH3	394.23
8.	Quinidine isovalerate	-OC(O)CH(CH3)2	408.24
9.	Quinidine tiglate	-OC(O)CH2CH(CH3)2	406.23
10.	Cinchonidine	-OH	294.17
11.	Cinchonidine butanoate	-OC(O)CH2CH2CH3	364.22
12.	Cinchonidine isobutanoate	-OC(O)CH(CH3)2	364.22
13.	Cinchonidine isovalerate	-OC(O)C(CHCH2)(CH3)	340.22
14.	Cinchonidine tiglate	-OC(O)CH2CH(CH3)2	376.22
15.	Cinchonine	-OH	337.18
16.	Cinchonine butanoate	-OC(O)CH2CH2CH3	364.22
17.	Cinchonine isovalerate	-OC(O)CH(CH3)2	357.27
18.	Cinchonine tiglate	-OC(O)CH2CH(CH3)2	376.22
19.	Hexyl quinine ether	-OC6H13	408.28
20.	Hexyl quinidine ether	-OC6H13	408.28
21.	Hexyl cinchonidine ether	-OC6H13	378.27
22.	Hexyl cinchonine ether	-OC6H13	378.27
23.	Isopropyl quinine ether	-OCH(CH3)2	366.23
24.	Isopropyl quinidine ether	-OCH(CH3)2	366.23
25.	Isopropyl cinchonine ether	-OCH(CH3)2	336.22

man P-glycoprotein.

Furthermore, we determine the chemical interaction that is involved in Cinchonidine isobutanoate (red) and hP-gp docking complex which has the best affinity energy (-8.6 kcal/mol). This interaction is stabilized by nine amino acid residues of the hP-gp present in the binding pocket, including Met-69, Pro-205, Tyr-307, Tyr-310, Phe-336, Phe-343, Gln-725, Phe-728, and Phe-732. The type of chemical interactions between amino acid residues of hP-gp with Cinchonidine isobutanoate involved hydrophobic interactions which could stabilize its binding mode.

According to molecular docking, Cinchonidine isobutanoate is the best candidate as anticancer from 30 designed molecules of Cinchona alkaloids derivatives.

This study will be used as a model for organic molecule synthesis and bioactive evaluation both in-vivo and in-vitro in the future [31, 32, 33] (Figure 3). In addition, Cinchonidine isobutanoate is ester derivative from cinchona alkaloids which has an isobutanoil group on its side chain as R-group. The inhibition constant (Ki) value of Cinchonidine isobutanoate is 4.89×10^{-7} M which indicates that Cinchonidine isobutanoate is the most efficient in inhibiting hP-gp over the other cinchona alkaloids. The inhibition constant (Ki) value is presented by the equation below:

$$\Delta G = -RT \ln K_A \quad ; \quad K_A = K_i^{-1} = \frac{[EI]}{[E][I]}$$

$$K_i = e^{\left(\frac{\Delta G}{RT}\right)}$$

Table 2. Binding energies and drug likeness properties of Cinchona alkaloids with hP-gp

| No.	Compound	Log P	Affinity Energy (Kcal/mol)	Violation of Lipinski`s Rule	Ki (M)
1.	Quinine	2.41	-7.6	0	2.65×10^{-6}
2.	Quinine butanoate	3.76	-6.9	0	8.64×10^{-6}
3.	Quinine isobutanoate	3.59	-8	0	1.35×10^{-6}
4.	Quinine isovalerate	4.18	-8.1	0	1.14×10^{-6}
5.	Quinine tiglate	4.22	-8	0	1.35×10^{-6}
6.	Quinidine	1.96	-8.4	0	6.85×10^{-7}
7.	Quinidine butanoate	3.85	-7.8	0	1.89×10^{-6}
8..	Quinidine isovalerate	4.18	-7.5	0	3.14×10^{-6}
9.	Quinidine tiglate	4.22	-7.7	0	2.24×10^{-6}
10.	Cinchonidine	2.32	-8.1	0	1.12×10^{-6}
11.	Cinchonidine butanoate	3.76	-8.4	0	6.86×10^{-7}
12.	Cinchonidine isobutanoate	3.5	-8.6	0	4.89×10^{-7}
13.	Cinchonidine isovalerate	4.1	-7.3	0	4.40×10^{-6}
14.	Cinchonidine tiglate	4.13	-7.1	0	6.16×10^{-6}
15..	Cinchonine	2.41	-8.5	0	2.49×10^{-7}
16.	Cinchonine butanoate	3.76	-7.7	0	2.49×10^{-7}
17.	Cinchonine isovalerate	4.68	-5.7	0	6.57×10^{-5}
18.	Cinchonine tiglate	4.13	-7.6	0	2.65×10^{-6}
19.	Hexyl quinine ether	5.27	-6.6	1	1.43×10^{-5}
20.	Hexyl quinidine ether	5.27	-7.3	1	4.40×10^{-6}
21.	Hexyl cinchonidine ether	5.18	-8.1	1	1.14×10^{-6}
22.	Hexyl cinchonine ether	5.18	-6.9	1	8.64×10^{-6}
23.	Isopropyl quinine ether	3.66	-7.6	0	2.65×10^{-6}
24.	Isopropyl quinidine ether	3.66	-7.4	0	3.71×10^{-6}
25.	Isopropyl cinchonine ether	3.57	-7.8	0	1.89×10^{-6}
26.	Isopropyl cinchonidine ether	3.57	-7.3	0	4.40×10^{-6}
27.	Buthyl quinine ether	4.3	-7.4	0	3.71×10^{-6}
28.	Buthyl quinidine ether	4.3	-8	0	1.35×10^{-6}
29.	Buthyl cinchonine ether	4.21	-7.8	0	1.89×10^{-6}
30.	Buthyl cinchonidine ether	4.21	-7.2	0	5.21×10^{-6}
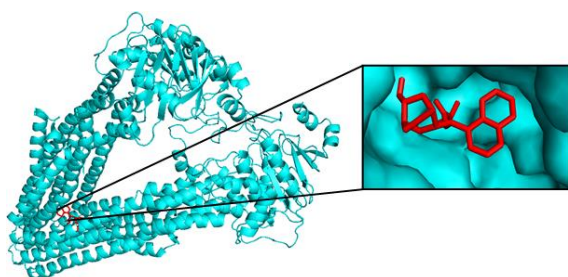
Figure 2.   Molecular docking interaction of hP-gp (cyan) and Cinchonidine isobutanoate (red)
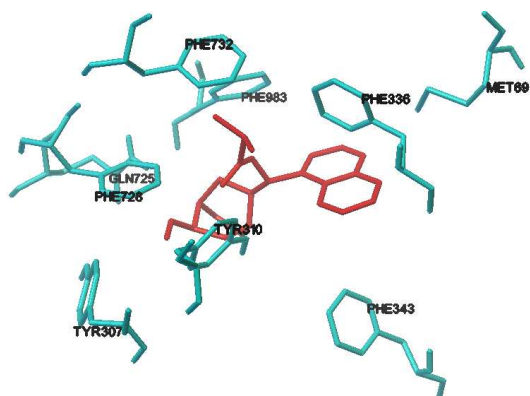

Figure 3.   Chemical interaction between Cinchonidine isobuta-noate (red) and hP-gp (cyan) complex

Here, we propose synthesis design of cinchona alkaloid which is less toxic and more active compared to cinchona parents (Figure 4). Dehydration reactions in water have been mediated by a surfactant-type catalyst, dodecylbenzene sulfonic acid (DBSA). These reactions include dehydrative esterification, etherification, thioesterification, and dithiol acetalization. In these reactions, DBSA and substrates form emulsion droplets where the interior side is hydrophobic enough to repel water molecules generated during the reactions [34, 35, 36]. Previous studies on the esterification-mediated surfactant catalyst showed that the yields of esters and ether quinine derivatives were affected by temperature, amounts of DBSA, and the substrates. Cinchona ester derivatives could be obtained in high yield under DBSA-catalyzed conditions and those compounds were also found proceeding smoothly. This work not only may lead to mild environmental systems but also will serve a new aspect of organic chemistry synthesis in water [35, 37, 38]. By utilizing an efficient, catalytic, rapid, stable and high-yielding protocol for the cinchona alkaloids synthesis by DBSA with amphipathic Brønsted acid, this will make commercially available, highly reactive, cheap, stable, excellent emulsifier and activator very powerful in obtaining pure high yields of synthesized product.
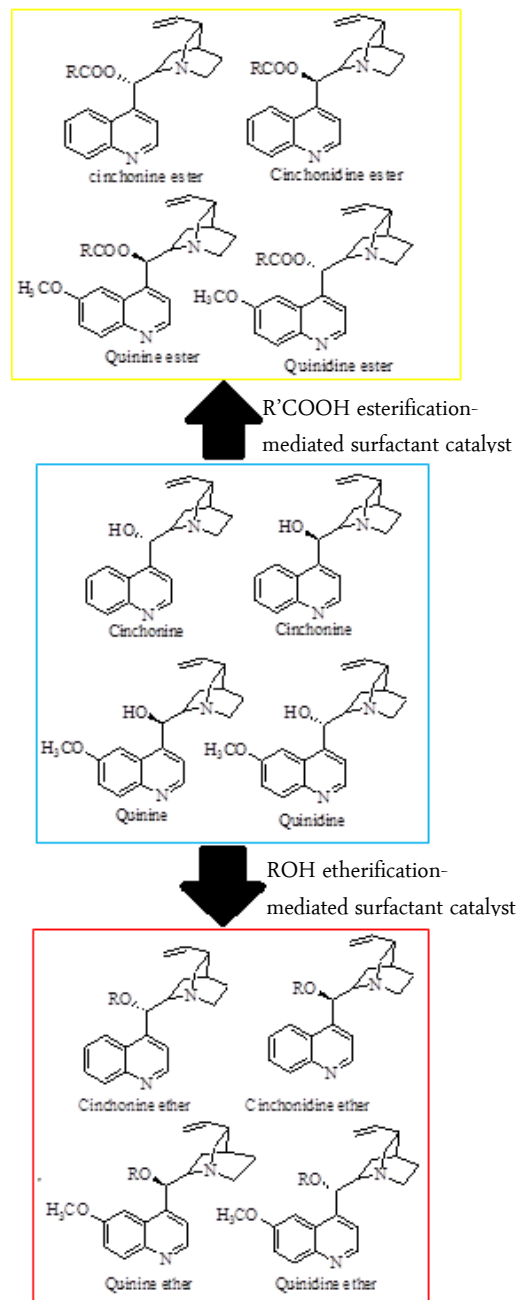

Figure 4.   Esterification and etherification reaction of cinchona alkaloids-mediated surfactant-type catalyst

CONCLUSION

In conclusion, a 3D model of human P-glycoprotein was successfully built through homology modeling. The energy affinity of potential cinchona alkaloids were evaluated by molecular docking approach. The molecular docking study revealed that Cinchonidine isobutanoate acts as the highest potent inhibitor upon hP-gp as they exhibit interaction with protein residues which present in the active site with high binding energy. Cinchonidine isobutanoate is proposed for further lead synthesis

by using DBSA, act as a combined Brønsted acid-surfactant-catalyst (BASC) to obtain a high concentration of organic product by forming mini emulsions which are powerful catalytic application in an aqueous solution.

ACKNOWLEDGMENT

REFERENCES

1. Callaghan R, Luk F, Bebawy M (2014) Inhibition of the multidrug resistance P-glycoprotein: Time for a change of strategy?. Drug Metabolism and Disposition 42 (4): 623-631. doi: 10.1124/dmd.113.056176.

2. Abdallah HM, Al-Abd AM, El-Dine RS, El-Halawany AM (2015) P-glycoprotein inhibitors of natural origin as potential tumor chemo-sensitizers: A review. Journal of Advanced Research 6 (1): 45-62. doi: 10.1016/j.jare.2014.11.008.

3. Davidson AL, Dassa E, Orelle C, Chen J (2008) Structure, function, and evolution of bacterial ATP-binding cassette systems. Microbiology Molecular and Biology Reviews 72 (2): 317-364. doi: 10.1128/MMBR.00031-07.

4. Vasiliou V, Vasiliou K, Nebert DW (2009) Human ATP-binding cassette (ABC) transporter family. Human Genomics 3 (3): 281-290. doi: 10.1186/1479-7364-3-3-281.

5. Solary E, Mannone L, Moreau D et al. (2000) Phase I study of cinchonine, a multidrug resistance reversing agent, combined with the CHVP regimen in relapsed and refractory lymphoproliferative syndromes. Leukemia 14 (12): 2085-2094.

6. Scagliotti GV, Novello S, Selvaggi G (1999) Multidrug resistance in non-small-cell lung cancer. Annals of Oncology 10 (Suppl 5): S83-86.

7. Merk J, Rolff J, Dorn C et al. (2011) Chemoresistance in non-small-cell lung cancer: can multidrug resistance markers predict the response of xenograft lung cancer models to chemotherapy? European Journal of Cardio-thorac Surgery 40 (1): e29-33. doi: 10.1016/j.ejcts.2011.02.010.

8. Peters GJ, Honeywell RJ (2015) Drug transport and metabolism of novel anticancer drugs. Expert Opinion on Drug Metabolism and Toxicology 11 (5): 661-663. doi: 10.1517/17425255.2015.1041255

9. Wang Y, Qi X, Li D et al. (2014) Anticancer efficacy and absorption, distribution, metabolism, and toxicity studies of aspergiolide A in early drug development. Drug Design, Development and Therapy 8: 1965-1977. doi: 10.2147/DDDT.

10. Kwon CH (1999) Metabolism-based anticancer drug design. Archives of Pharmacal Research 22 (6): 533-541. doi: 10.1007/BF02975322.

11. Slordal L, Aarbakke J (1987) Effect of anticancer drugs on drug metabolism. Pharmacology and Therapeutics 35 (1-2): 217-226. doi: 10.1016/0163-7258(87)90107-0.

12. Szewczyk P, Tao H, McGrath AP et al. (2015) Snapshots of ligand entry, malleable binding and induced helical movement in P-glycoprotein. Acta Crystallographica D 71 (Pt 3): 732-741. doi: 10.1107/S1399004715000978.

13. Jin MS, Oldham ML, Zhang Q, Chen J (2012) Crystal structure of the multidrug transporter P-glycoprotein from *Caenorhabditis elegans*. Nature 490 (7421):566-559. doi:10.1038/nature11448.

14. Li J, Jaimes KF, Aller SG (2014) Refined structures of mouse P-glycoprotein. Protein Science 23 (1): 34-46. doi: 10.1002/pro.2387.

15. Biasini M, Bienert S, Waterhouse A et al. (2014) SWISS-MODEL: modelling protein tertiary and quaternary structure using evolutionary information. Nucleic Acids Research 42 (Web Server issue): W252-258. doi: 10.1093/nar/gku340.

16. Bordoli L, Kiefer F, Arnold K et al. (2009) Protein structure homology modeling using SWISS-MODEL workspace. Nature Protocols 4 (1): 1-13. doi: 10.1038/nprot.2008.197.

17. Arnold K, Bordoli L, Kopp J, Schwede T (2006) The SWISS-MODEL workspace: a web-based environment for protein structure homology modelling. Bioinformatics 22 (2): 195-201. doi: 10.1093/bioinformatics/bti770

18. Schwede T, Kopp J, Guex N, Peitsch MC (2003) SWISS-MODEL: An automated protein homology-modeling server. Nucleic Acids Research 31 (13): 3381-3385.

19. Laskowski RA, Rullmannn JA, MacArthur MW et al. (1996) AQUA and PROCHECK-NMR: programs for checking the quality of protein structures solved by NMR. Journal of Biomolecular NMR 8 (4): 477-486. doi: 10.1007/BF00228148.

20. Carugo O, Djinovic-Carugo K (2013) A proteomic Ramachandran plot (PRplot). Amino Acids 44 (2): 781-790. doi: 10.1007/s00726-012-1402-z.

21. Gopalakrishnan K, Sowmiya G, Sheik SS, Sekar K. Ramachandran plot on the web (2.0). Protein and Peptide Letters 14 (7): 669-671. doi: 10.2174/092986607781483912.

22. Ho BK, Thomas A, Brasseur R (2003) Revisiting the Ramachandran plot: hard-sphere repulsion, electrostatics, and H-bonding in the alpha-helix. Protein Science 12 (11): 2508-2522. doi: 10.1110/ps.03235203.

23. Kolaskar AS, Sawant S (1996) Prediction of conformational states of amino acids using a Ramachandran plot. Chemical Biology and Drug Design 47 (1-2): 110-116. doi: 10.1111/j.1399-3011.1996.tb00817.x.

24. Colovos C, Yeates TO (1993) Verification of protein structures: patterns of nonbonded atomic interactions. Protein Science 2 (9): 1511-1519. doi: 10.1002/pro.5560020916.

25. Cousins KR (2011) Computer review of ChemDraw Ultra 12.0. Journal of the American Chemical Society 133 (21): 8388. doi: 10.1021/ja204075s.

26. Li Z, Wan H, Shi Y, Ouyang P (2004) Personal experience with four kinds of chemical structure drawing software: review on ChemDraw, ChemWindow, ISIS/Draw, and ChemSketch. Journal of Chemical Information and Modeling 44 (5): 1886-1890. doi: 10.1021/ci049794h.

27. Southan C, Stracz A (2013) Extracting and connecting chemical structures from text sources using chemicalize.org. Journal of Cheminformatics 5 (1): 20. doi: 10.1186/1758-2946-5-20.

28. Fernandez-Recio J, Totrov M, Abagyan R (2002) Screened charge electrostatic model in protein-protein docking simulations. Pacific Symposium on Biocomputing 2002: 552-563.

29. Sharom FJ (2011) The P-glycoprotein multidrug transporter. Essays Biochem 50 (1): 161-178. doi: 10.1042/bse0500161.

30. Kadioglu O, Saeed ME, Valoti M et al. (2016) Interactions of human P-glycoprotein transport substrates and inhibitors at the drug binding domain: Functional and molecular docking analyses. Biochemical Pharmacology 104: 42-51. doi: 10.1016/j.bcp.2016.01.014.

31. Follit CA, Brewer FK, Wise JG, Vogel PD (2015) *In silico* identified targeted inhibitors of P-glycoprotein overcome multidrug resistance in human cancer cells in culture. Pharmacology Research and Perspectives 3 (5): e00170. doi: 10.1002/prp2.170.

32. Aller SG, Yu J, Ward A et al. (2009) Structure of P-glycoprotein reveals a molecular basis for poly-specific drug binding. Science 323 (5922): 1718-1722. doi: 10.1126/science.1168750.

33. Badhan R, Penny J (2006) *In silico* modelling of the interaction of flavonoids with human P-glycoprotein nucleotide-binding domain. European Journal of Medicinal Chemistry 41 (3): 285-295. doi: 10.1016/j.ejmech.2005.11.012.

34. Akiyama T, Mori K (2015) Stronger bronsted acids: Recent progress. Chemical Reviews 115 (17): 9277-9306. doi: 10.1021/acs.chemrev.5b00041.

35. Shirakawa S, Kobayashi S (2007) Surfactant-type Bronsted acid catalyzed dehydrative nucleophilic substitutions of alcohols in water. Organic Letters 9 (2): 311-314. doi: 10.1021/ol062813j.

36. Hiroto S, Shinokubo H, Osuka A (2006) Porphyrin synthesis in water provides new expanded porphyrins with direct bipyrrole linkages: isolation and characterization of two heptaphyrins. Journal of the American Chemical Society 128 (20): 6568-6569. doi: 10.1021/ja061621g.

37. Manabe K, Iimura S, Sun XM, Kobayashi S (2002) Dehydration reactions in water. Bronsted Acid-surfactant-combined catalyst for ester, ether, thioether, and dithioacetal formation in water. Journal of the American Chemical Society 124 (40): 11971-11978. doi: 10.1021/ja026241j

38. Gogoi P, Hazarika P, Konwar D (2005) Surfactant/I2/water: an efficient system for deprotection of oximes and imines to carbonyls under neutral conditions in water. The Journal of Organic Chemistry 70 (5): 1934-1936. doi: 10.1021/jo0480287.